Plunge Milling Force Model using Instantaneous Cutting Force Coefficients

Jeong Hoon Ko[1,#]

1 Department of Mechanical Engineering, The University of British Columbia, Vancouver, Canada
Corresponding Author / E-mail:jhko5889@yahoo.com, TEL: +01-604-827-5007, FAX: +01-604-822-2403

KEYWORDS : Plunge milling process, Cutting force model, Uncut chip thickness, Nonlinear cutting force coefficients

Plunge milling process is used for machining hole and is widely used in aerospace, automobile, and die/mold industries. The cutter is fed in the direction of spindle axis which has the highest structural rigidity. The kinematics of plunge milling differs from the traditional turning and milling in aspect of tool engagement and chip generation. This paper proposes the mechanistic cutting force model for plunge milling. Uncut chip thickness is calculated using the present cutter edge position and the previous cutter edge position. Instantaneous cutting force coefficients, which depend only on instantaneous uncut chip thickness, are derived based on the mechanistic approach. The developed cutting force model is verified through comparison of the predicted and the measured cutting forces.

Manuscript received: April 8, 2005 / Accepted: November 11, 2005

NOMENCLATURE

l = insert length
R = radius
d_x = offset in x direction
d_y = offset in y direction
d_z = offset in z direction
λ = axial rake angle
η = radial rake angle of boundary cutting edge
α = radial rake angle of cutting edge
β = cutting edge angle
ϕ_p = pitch angle
$F_n(i,j,k)$ = normal pressure force
$F_f(i,j,k)$ = frictional force
$\vec{\tau}$ = unit vector tangent to the cutter edge
$\vec{n}$ = unit vector normal to rake face
$\vec{b}$ = unit vector on the rake surface and perpendicular to $\vec{\tau}$
$\vec{T}_c$ = chip flow vector
N_f =the number of flutes
Δa = length of edge element along radial direction.
N_a = total disk number
θ = rotation angle of the cutter
ϕ = cutting edge location angle
$T(\phi)$ = transformation matrix
ϕ_c = flute spacing angle
t_c = uncut chip thickness
t_{cr} = rescaled uncut chip thickness
ds = cutting edge length
K_n = normal cutting force coefficients
K_f = frictional cutting force coefficients
θ_c = chip flow angle

1. Introduction

The plunge milling process shown in Fig. 1 is very suitable for machining wide hole and is widely used in aerospace, automobile, and die/mold industries. The kinematics of plunge milling differs from that of traditional turning and milling in aspect of tool engagement and chip generation. Wakaoka, S. *et al.* studied on design of plunge milling cutter to make vertical walls with high accuracy and high speed.[1] Li, S. *et al.* performed research on plunge cutting to create complicated chamfer pattern.[2] However, there have been no research results about plunge milling force model, which can predict cutting force for general plunge milling process with unsymmetrical cutter geometry.

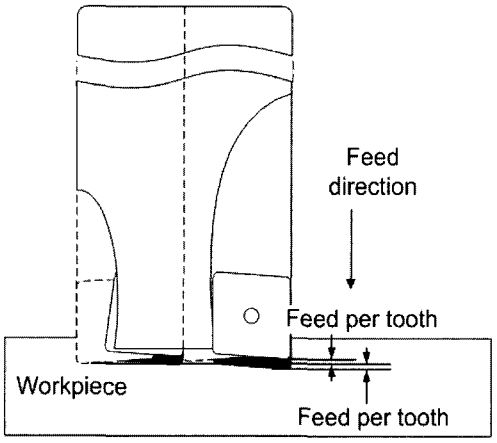

Fig. 1 Plunge milling process

The cutting forces need to be estimated to select the cutting conditions for plunge milling and to physically verify the NC code.[3]

This paper presents a plunge milling force model including instantaneous uncut chip thickness model and cutting force coefficients model based on mechanistic approach. Especially, instantaneous cutting force coefficients are applied to increase accuracy and decrease the number of calibration.[4] Finally, the predicted cutting force is compared to the measured one.

2. Formulation of Mechanistic Cutting Force Model

Since only the bottom flutes of a plunge mill are involved in plunge milling, this paper focuses on modeling of the cutting force generated by the bottom flutes. Bottom flutes of a plunge mill can be divided into a finite number of disk elements along radial direction. The total *x*-, *y*-, and *z*-force components acting on a flute at a particular instant are obtained by numerically integrating the force components acting on each individual disk element. The total force acting on a cutter at a given time is determined by summing the force acting over all of the flutes engaged in cutting.

Fig. 2 shows the geometry of the plunge mill. When two inserts are fixed into cutter body, the geometry of two flutes is illustrated in Fig. 2. The geometry variables of the plunge mill used in this paper have the specific values presented in Table 1. The helix angle and rake angle of the bottom flute is 0 deg. and 5 deg., respectively.

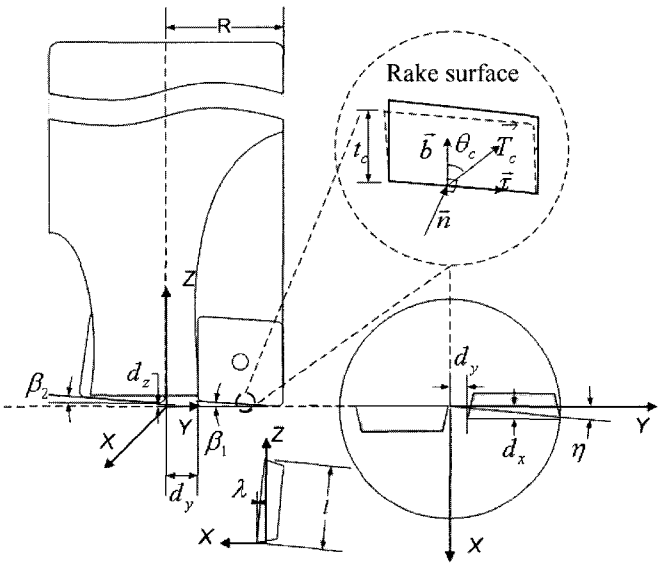

Fig. 2 Plunge mill geometry

Table 1 The geometry for the insert and the flutes of the plunge mill

Insert length l	12.700 mm	Axial rake angle λ	5 deg.
Cutter radius R	15.875 mm	Cutting edge angle β_1	4 deg.
Offset d_x	1.659 mm	Cutting edge angle β_2	2 deg.
Offset d_y	3.175 mm	Radial rake angle of boundary cutting edge η	6 deg.
Offset d_z	0.270 mm		

Fig. 3 shows the variables for definition of angular positions. The angular position of the k^{th} disk element of the i^{th} flute at the j^{th} angular position of the cutter is described by

$$\phi(i,j,k) = \psi(i,j) + \alpha(i,k) \quad (1)$$

$$\psi(i,j) = \theta(j) + (i-1)\phi_c \quad (2)$$

$$\theta(j) = -j\Delta\theta \quad (3)$$

where ψ is used to define the rotation angle from zero angular position to the line of each flute passing through the center of the cutter. α is a radial rake angle and is defined as the deviation angle of each edge element from the line passing through the center of the cutter. θ shows the rotation angle of the cutter and ϕ_c is the flute spacing angle.

In case of the 1st bottom flute, a radial rake angle $\alpha(k)$ can be calculated as follows:

$$\alpha(k) = \tan^{-1}(R\cdot\sin(\eta)/(d_y + k\Delta a + \frac{\Delta a}{2}))) \quad (4)$$
$$d_y = R - IW$$

where d_y is the offset in y direction and Δa is the height of the axial disk element.

In case of the 2nd bottom flute, $\alpha(k) = 0$, $d_y = 0$

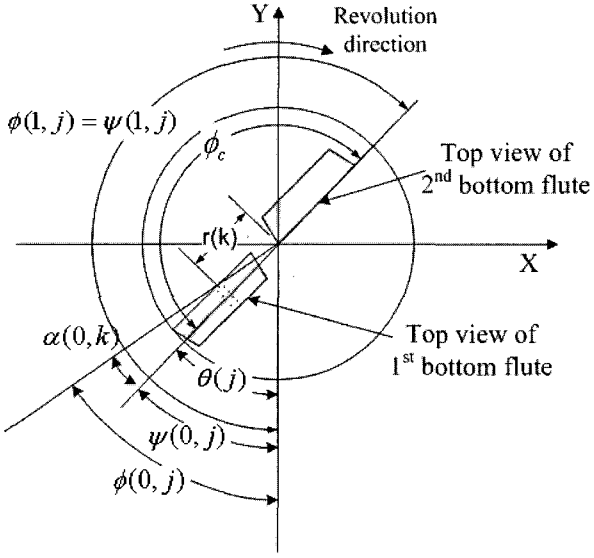

Fig. 3 The variable for definition of angular position

The unit vectors ($\vec{n}, \vec{T}_c, \vec{\tau}, \vec{b}$) on the rake surface must be derived to build a cutting force model. First, the edge unit vectors for a rake angle of λ are determined assuming that edge rotation angles (ψ) are zero. Then the unit vectors for the real edge rotation angle ψ are derived using the transformation matrix ($T(\psi)$).

The unit vector $\vec{n}$ for a bottom edge with axial rake angle λ is defined as

$$\vec{n} = \cos\lambda\vec{i} - \sin\lambda\vec{k} \quad (5)$$

$\vec{\tau}$ is the unit vector tangent to the helical cutter edge, expressed as

$$\vec{\tau} = \frac{d\vec{r}}{\|d\vec{r}\|} \quad (6)$$

where $d\vec{r}$ is the derivative of $\vec{r}$, which is the vector from the origin of the cutter coordinate system to the rake surface of flute 1 in Fig. 3.[4] When edge rotation angle is zero, $\vec{r}$ is defined as

$$\vec{r} = x\vec{i} + y\vec{j} + z\vec{k} \quad (7)$$

where, in case of the 1st bottom flute, x, y, and z coordinates can be calculated as follows:

$$x = -d_x = -R\sin\eta,\ y = -(k\cdot\Delta a + d_y),$$
$$z = (R - (k\cdot\Delta a + d_y))\cdot\tan\beta_1 \quad (8)$$

And, in case of the 2nd bottom flute, x, y, and z coordinates can be calculated as follows:

$$x = 0,\quad y = -k\cdot\Delta a,\quad z = k\cdot\Delta a\cdot\tan\beta_2 + d_z \quad (9)$$

Thus, $\vec{\tau}(k)$ can be defined as follows:

$$\vec{\tau}(k) = \frac{d\vec{r}}{\|d\vec{r}\|} = \frac{dy\vec{j} + dz\vec{k}}{\sqrt{dy^2 + dz^2}} = \frac{(dy/dk)\vec{j} + (dz/dk)\vec{k}}{\sqrt{(dy/dk)^2 + (dz/dk)^2}} = \frac{1}{f_2}\vec{j} + \frac{f_1}{f_2}\vec{k} \quad (10)$$

where f_1 and f_2 of the 1st bottom flute are defined as follows:

$$f_1 = \tan\beta_1 \quad f_2 = -\sqrt{f_1^2 + 1} \quad (11)$$

And f_1 and f_2 of the 2nd bottom flute are defined as follows:

$$f_1 = -\tan\beta_2 \quad f_2 = -\sqrt{f_1^2 + 1} \quad (12)$$

Since $\vec{b}$ is a unit vector on the rake surface and perpendicular to $\vec{\tau}$, the unit vector $\vec{b}$ is

$$\vec{b} = \vec{\tau} \times \vec{n} = \frac{1}{f_2}(-\vec{i}\sin\lambda + \vec{j}\cdot f_1\cos\lambda - \vec{k}\cos\lambda) \quad (13)$$

Chip flow vector $\vec{T}_c$ is defined by combination of $\vec{\tau}$ and $\vec{b}$, as shown in Fig. 2:

$$\vec{T}_c = \cos\theta_c\vec{b}(\alpha) + \sin\theta_c\vec{\tau}(\alpha) \quad (14)$$

$\vec{T}_c$ can be determined by substituting Eqs. (10) and (3) into Eq. (14):

$$\vec{T}_c = \cos\theta_c\vec{b} + \sin\theta_c\vec{\tau} = \frac{1}{f_2}(\vec{i}(-\cos\theta_c\sin\lambda) + \vec{j}(f_1\cos\theta_c\cos\lambda + \sin\theta_c) + \vec{k}(-\cos\lambda\cos\theta_c + f_1\sin\theta_c)) \quad (15)$$

The cutting force acting on the rake surface of a disk element is divided into two orthogonal components: the normal pressure force, $F_n(i,j,k)$, and the frictional force, $F_f(i,j,k)$. It can be obtained from

$$F_n(i,j,k) = K_n\vec{n}T(\psi)dA_c \quad (16)$$

$$F_f(i,j,k) = K_fK_n\vec{T}_cT(\psi)dA_c \quad (17)$$

where $dA_c = t_c(\phi)\cos\alpha_r(\Delta a)$, and $\vec{n}$ and $\vec{T}_c$ are the unit vectors defined in Eqs. (5) and (15), respectively.

$T(\psi)$ is the transformation matrix for rotating the edge according to edge location angle ϕ and can be defined as follows:

$$T(\psi) = \begin{bmatrix} \cos\psi & -\sin\psi & 0 \\ \sin\psi & \cos\psi & 0 \\ 0 & 0 & 1 \end{bmatrix} \quad (18)$$

Finally, F_n and F_f can be decomposed into three orthogonal force components in Cartesian coordinates by substituting Eqs. (5), (14), and (18) into Eqs. (16) and (17), and can be derived into

$$F_x(i,j,k) = [K_n(\cos\phi\cos\lambda) + K_nK_f\cos\theta_c\frac{1}{f_2}(-\cos\phi\sin\lambda - f_1\cos\lambda\sin\phi) + K_nK_f\sin\theta_c\frac{1}{f_2}(-\sin\phi)]dA_c \quad (19)$$

$$F_y(i,j,k) = [K_n(\sin\phi\cos\lambda) + K_nK_f\cos\theta_c\frac{1}{f_2}(-\sin\phi\sin\lambda + f_1\cos\phi\cos\lambda) + K_nK_f\sin\theta_c\frac{1}{f_2}(\cos\phi)]dA_c \quad (20)$$

$$F_z(i,j,k) = [K_n(-\sin\lambda) + K_nK_f\cos\theta_c\frac{1}{f_2}(-\cos\lambda) + K_nK_f\sin\theta_c\frac{1}{f_2}(f_1)]dA_c \quad (21)$$

3. Uncut chip thickness model

The uncut chip thickness is defined as the distance between the path that the current tooth of intersect is generating, and the exposed workpiece surface that a previously passing tooth has generated. The uncut chip thickness is calculated following cutter edge position determined by feed per tooth(f_t) and the edge angular position.

In case of the 1st bottom flute, x, y, and z coordinates can be calculated as follows:

$$x = -R\sin\eta\cos\phi + (k\Delta a + d_y)\sin\phi \quad (22)$$

$$y = -R\sin\eta\sin\phi - (k\cdot\Delta a + d_y)\cos\phi \quad (23)$$

$$z = (R - (k\cdot\Delta a + d_y))\cdot\tan\beta_1 - \frac{\theta}{2\pi}N_f f_t \quad (24)$$

In case of the 2nd bottom flute, x, y, and z coordinates can be calculated as follows:

$$x = k\Delta a\sin\phi \quad (25)$$

$$y = -k\cdot\Delta a\cos\phi \quad (26)$$

$$z = k\cdot\Delta a\cdot\tan\beta_2 - \frac{\theta}{2\pi}N_f f_t \quad (27)$$

In plunge milling, the uncut chip thickness is generated by difference between z position of the present edge and that of the previously passed one at the same edge location angle. When the present cutter edge location angle of the k^{th} edge disk element of cutter edge is ϕ, the uncut chip thickness generated in the disk element is calculated as:

$$t_{cm}(i,j,k,m) = z_m - z \quad ,$$
$$t_c(z) = Max[0, Min(t_{cm}(i,j,k,m))] \quad (28)$$

where $t_{cm}(i, j, k, m)$ represents the possible uncut chip thicknesses, z_m is the z coordinate of the cutting edge in previously passed teeth (m = 1 , ..., N_f) at the same edge location angle as the present edge location angle ϕ , and t_c the real uncut chip thickness.

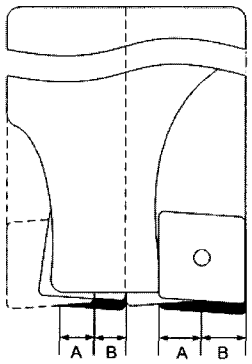

(a)Uncut chip thickness distribution

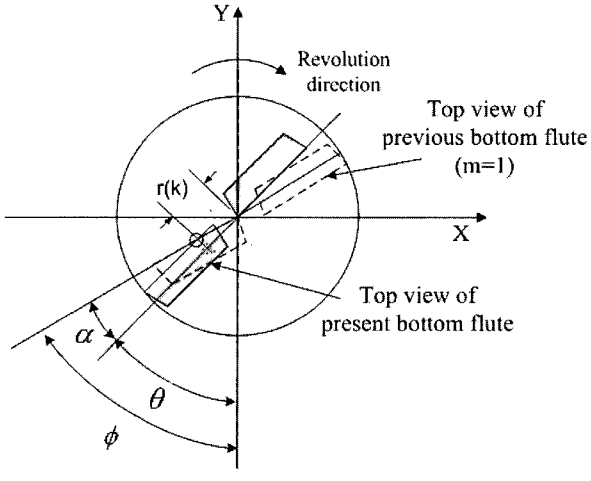

(b) Configuration for calculation of uncut chip thickness

Fig. 4 Uncut chip thickness for plunge milling

Fig. 4 shows uncut chip thickness generated in plunge mill with two flutes. In A section, the uncut chip thickness is generated by the present flute edge and the previously passed flute edge when m is 1. In B section, uncut chip thickness is generated by the present flute edge and the previously passed flute edge when m is 2.

For example, Fig. 4(b) illustrates the configuration when uncut chip thickness is generated by the first bottom flute at r(k). In this case, z position of the present flute edge element at r(k) can be calculated as follows:

$$z = (R - (k \cdot \Delta a + d_y)) \cdot \tan\beta_1 - \frac{\theta}{2\pi} N_f f_t \tag{29}$$

And z position of the previous flute edge element (m=1) at r(k) can be calculated as follows:

$$z_1 = k \cdot \Delta a \cdot \tan\beta_2 - \frac{\theta - \phi_c + \alpha}{2\pi} N_f f_t \tag{30}$$

In the above equation, α is given in Eq. (4) and $-\phi_c + \alpha$ shows the difference of rotation angle between the present edge and the previously passed one when m is 1.

The other possible uncut chip thickness can be generated between the present flute edge and the previously passed flute edge element when m is 2. In this case, the difference of rotation angle between two edges is $2\phi_c$. Therefore, z position of the previous flute edge element at r(k) can be calculated as follows:

$$z_2 = (R - (k \cdot \Delta a + d_y)) \cdot \tan\beta_1 - \frac{\theta - 2\phi_c}{2\pi} N_f f_t \tag{31}$$

Then, two possible uncut chip thicknesses are calculated as follows:

$$t_{c1} = z_1 - z \quad , t_{c2} = z_2 - z \tag{32}$$

Finally, the real uncut chip thickness can be estimated as follows:

$$t_c(z) = Max[0, Min(t_{c1}, t_{c2})] \tag{33}$$

If r(k) is within A section, uncut chip thickness is calculated as t_{c1}. Otherwise, uncut chip thickness is t_{c2}. The above procedure can be applied for calculation of uncut chip thickness generated by the second bottom flute.

4. Determination of Cutting Force Coefficients

Fig. 5 shows the cutting configurations to calculate cutting force coefficients. Cutting forces generated by plunge mill with one insert is used to calibrate cutting force coefficients. In this cutting configuration, the uncut chip thickness is the same as feed per tooth.

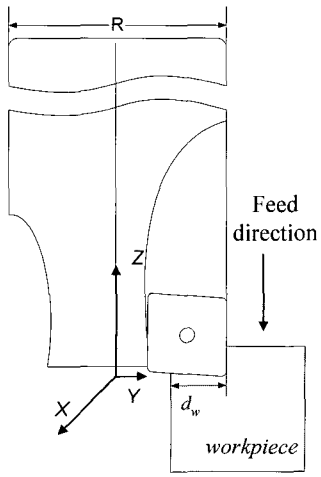

Fig. 5 The cutting configuration for calibration of cutting force coefficients

The cutting force coefficients can be calculated using the measured cutting forces F_x, F_y, F_z and uncut chip thickness f_t. The summation of cutting force equation Eqs. (19), (20), and (21), can be rewritten into matrix form as:

$$\begin{Bmatrix} F_x \\ F_y \\ F_z \end{Bmatrix} = \begin{bmatrix} A_{11} & A_{12} & A_{13} \\ A_{21} & A_{22} & A_{23} \\ A_{31} & A_{32} & A_{33} \end{bmatrix} \begin{Bmatrix} K_1 \\ K_2 \\ K_3 \end{Bmatrix} \tag{34}$$

where

$$A_{11} = B_1 \sum_k \sum_i (\cos\phi \cos\lambda) \cdot t_c(\phi)$$

$$A_{12} = B_1 \sum_k \sum_i \frac{1}{f_2}(-\cos\phi \sin\lambda - f_1 \cos\lambda \sin\phi) \cdot t_c(\phi)$$

$$A_{13} = B_1 \sum_k \sum_i \frac{1}{f_2}(-\sin\phi) \cdot t_c(\phi)$$

$$A_{21} = B_1 \sum_k \sum_i (\sin\phi \cos\lambda) \cdot t_c(\phi)$$

$$A_{22} = B_1 \sum_k \sum_i \frac{1}{f_2}(-\sin\phi \sin\lambda + f_1 \cos\phi \cos\lambda) \cdot t_c(\phi),$$

$$A_{23} = B_1 \sum_k \sum_i \frac{1}{f_2}(\cos\phi) \cdot t_c(\phi),$$

$$A_{31} = B_1 \sum_k \sum_i (-\sin\lambda) \cdot t_c(\phi)$$

$$A_{32} = B_1 \sum_k \sum_i \frac{1}{f_2}(-\cos\lambda) \cdot t_c(\phi)$$

$$A_{33} = B_1 \sum_k \sum_i \frac{1}{f_2}(f_1) \cdot t_c(\phi) \quad \text{and} \quad B_1 = \cos\lambda(\Delta a / \cos\alpha)$$

$$K_1 = K_n, \quad K_2 = \cos\theta_c K_n K_f \quad \text{and} \quad K_3 = \sin\theta_c K_n K_f$$

K_1, K_2, and K_3 can be obtained from the measured cutting force values using Cramer's Rule. The values of K_n, K_f, and θ_c are then readily calculated using

$$K_n = K_1, \quad \theta_c = \tan^{-1}\left(\frac{K_3}{K_2}\right), \quad K_f = \frac{K_2}{\cos\theta_c K_1} \tag{35}$$

Table 2 Cutting conditions (Tool : ECMPR202W20 Dia = 1.25 in (31.75 mm), Workpiece Material: Al6061, Spindle speed = 1000 rpm)

No.	Number of inserts(N_f) / Width of cut (d_w mm)	Feed per tooth (mm/tooth)
1	2/31.75	0.0125
2		0.0250
3		0.0375
4		0.01875
5		0.03125
6	1/ 11	0.0050
7		0.0100
8		0.0200
9		0.0250
10		0.0300
11		0.0400
12		0.0450
13		0.0500

Table 2 shows the cutting condition to obtain cutting force coefficients and verify the cutting force model. The cutting force coefficients are calibrated from the cutting forces measured from Tests 6, 7, 8, and 13. The cutting force coefficient models for a plunge milling are based on mechanistic approach using instantaneous cutting forces and instantaneous uncut chip thickness. When the summation of the uncut chip thickness approaches the maximum value at the specific rotation angle, the cutting force F_z also becomes the maximum value. Using this synchronization process, cutting force coefficients can be calculated with the feed per tooth and the

instantaneous cutting forces F_x, F_y and F_z at the specific rotation angle where the maximum F_z is generated. The measured instantaneous cutting forces F_x, F_y and F_z are inputted to left side column of Eq. (34) and the feed per tooth is given to Matrix [A] of Eq. (34). Finally, instantaneous cutting force coefficient is calculated using Cramer's Rule and Eq. (35).

$\ln(K_n)$ is plotted against the rescaled uncut chip thickness ($t_{cr}(i, j, k)$), which is defined as

$$t_{cr}(i,j,k) = \frac{t_c(i,j,k)}{ds(k)/\Delta a} \tag{36}$$

where $ds(k)$ is the length of the cutting edge at the k^{th} bottom disk element in radial direction. This compensates for the effects of ds[4].

The relationship between the rescaled uncut chip thickness $t_{cr}(i, j, k)$ and $\ln(K_n)$ can readily be derived using the Weibull function.

$$\ln(K_n) = A_1 - (A_1 - A_2)e^{-(A_3 t_{cr})^{A_4}} \tag{37}$$

K_f and θ_c can be represented as the nonlinear function dependent only on instantaneous uncut chip thickness $t_c(i, j, k)$ as [4]:

$$K_f = B_1 - (B_1 - B_2)e^{-(B_3 t_c)^{B_4}} \tag{38}$$

$$\theta_c = \frac{C_1 - C_2}{1 + (t_c / C_3)^{C_4}} + C_2$$

Table 3 Estimated cutting force coefficients

Workpiece Material	K_n (N/mm^2)	K_f	θ_c (rad.)
Al6061	A_1 = 6.800 A_2 = 9.855 A_3 = 0.819 A_4 = 0.543	B_1 = 0.882 B_2 = 1.262 B_3 = 0.287 B_4 = 1.194	C_1 = 0.386 C_2 =-0.458 C_3 = 5.306 C_4 = 0.642

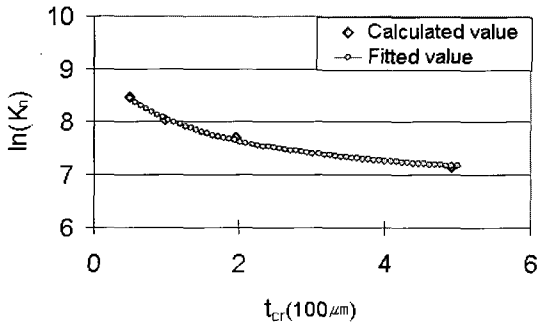

(a)Plot of $\ln(K_n)$ versus the rescaled uncut chip thickness (t_{cr})

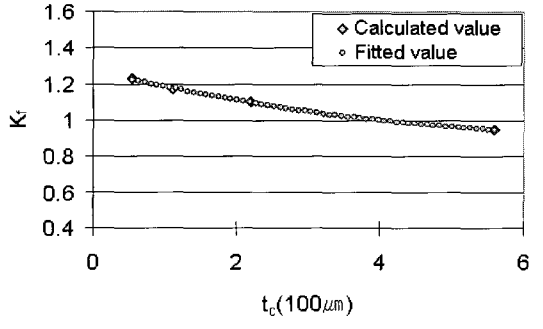

(b) Plot of K_f versus the instantaneous uncut chip thickness (t_c)

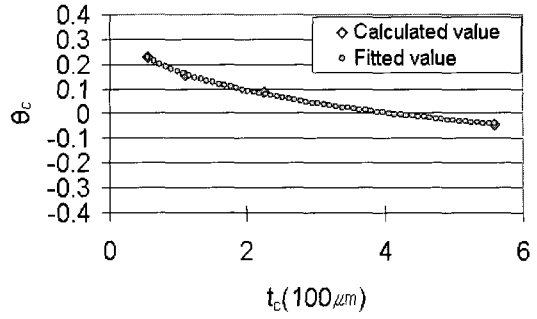

(c) Plot of θ_c versus the instantaneous uncut chip thickness (t_c)

Fig. 6 Plot of cutting force coefficients

Table 3 shows the calculated values of cutting force coefficient parameters using the explained method. Fig. 6 shows the cutting force coefficients obtained from Tests 6, 7, 8 and 13 and the fitted values. Cutting force coefficients increase at small uncut chip thicknesses, which is the typical behavior of the size effect phenomenon. Also it can be seen that the presented model fits the values well.

5. Model Validation

The 3D cutting forces were predicted using the determined cutting force coefficient under cutting conditions that differed from those used in the calibration tests. Fig. 7 shows the measured and predicted cutting forces under various cutting conditions. Fig. 7(a) and 7(b) show the cutting force generated under the cutting configuration shown in Fig. 5. Fig. 7 (c) and 7(d) illustrate the cutting force generated under the cutting configuration with two flute as shown in Fig. 4(a). It can be known from Fig. 7(c) and 7(d) that, if two flutes get involved in machining, cutting forces F_x and F_y are reduced because most of F_x and F_y generated by each flute is cancelled each other. In case of fully immersed plunge milling process, cutting force F_z doesn't change according to cutter rotation angle. F_z equation from Eq. (34) can be expressed as follows:

$$F_z = A_{31}K_1 + A_{32}K_2 + A_{33}K_3 \tag{39}$$

where

$$A_{31} = B_1 \sum_k \sum_i (-\sin\lambda) \cdot t_c(\phi),\ A_{32} = B_1 \sum_k \sum_i \frac{1}{f_2}(-\cos\lambda) \cdot t_c(\phi),$$
$$A_{33} = B_1 \sum_k \sum_i \frac{1}{f_2}(f_1) \cdot t_c(\phi)$$

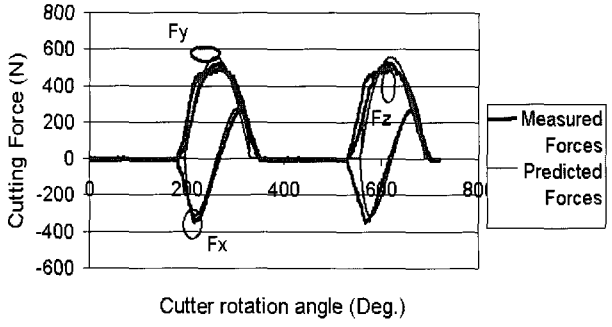

(a)Cutting conditions: feed rate = 25 mm/min, feed per tooth = 0.025 (Test 9)

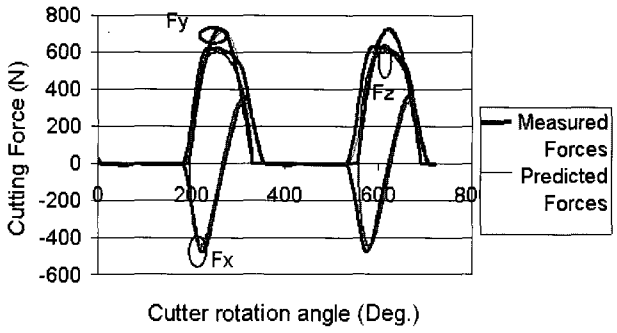

(b)Cutting conditions: feed rate = 45 mm/min, , feed per tooth = 0.045 (Test 12)

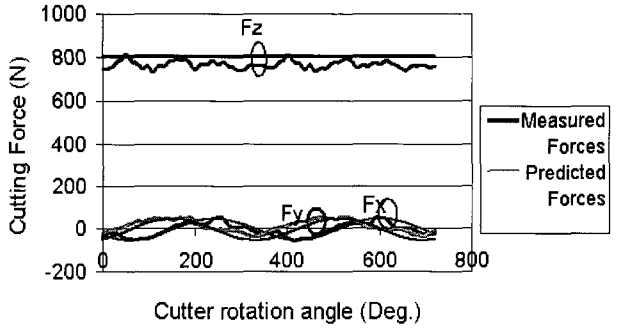

(c)Cutting conditions: feed rate = 25 mm/min, feed per tooth = 0.0125 (Test 1)

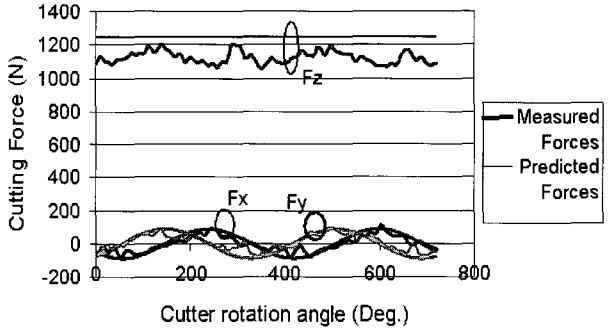

(d)Cutting conditions: feed rate = 75 mm/min, feed per tooth = 0.0375 (Test 3)

Fig. 7 Comparison of measured and predicted cutting forces for fixed cutting conditions

Eq.(39) shows that only the uncut chip thickness $t_c(\phi)$ depends on the cutter rotation angle and, in case of fully immersed cutting condition, the summation of $t_c(\phi)$ doesn't change according to cutter rotation angle because all the cutting edges are always engaged in workpiece. Therefore, F_z is found to be constant in case of fully immersed cutting condition as shown in Figs. 7(c) and 7(d).

There is good agreement in both the magnitude and shape of the predicted and measured forces, with a maximum prediction error of 9%.

6. Conclusion

In this paper, a cutting force model for plunge milling was developed to facilitate the cutting condition planning in light of the optimization of cutting process. The cutting force coefficient model was presented as function independent of cutting conditions. With a few calibration tests, cutting force coefficients were obtained based on mechanistic approach. The agreement between the predicted and measured cutting forces was excellent with a maximum error of 9 %. Without performing a number of calibration tests, the proposed cutting force model made it possible to predict the cutting force in plunge milling accurately.

ACKNOWLEDGEMENT

This work was supported by the Post-doctoral Fellowship Program of Korea Research Foundation (KRF).

REFERENCES

1. Wakaoka, S., Yamane, Y., Sekiya, K. and Narutaki, N., "High-speed and high-accuracy plunge cutting for vertical walls," Journal of Materials Processing Technology, Vol. 127, No. 2, pp. 246-250, 2002.

2. Li, Y., Liang, S. Y., Petrof, R. C. and Seth, B. B., "Force Modelling for Cylindrical Plunge Cutting," International Journal of Advanced Manufacturing Technology, Vol. 16, No. 12, pp. 863-870, 2004.

3. Altintas, Y., "Manufacturing Automation: Metal Cutting Mechanics, Machine Tool Vibrations, and CNC Design," Cambridge University Press, 2000.

4. Ko, J. H. and Cho, D. W., "3D Ball-End Milling Force Model Using Instantaneous Cutting Force Coefficients," Transactions of the ASME, Journal of Manufacturing Science and Engineering, Vol. 127, No. 1, pp. 1-12, 2005.